Environmental Science and Pollution Research (2022) 29:76456–76471
https://doi.org/10.1007/s11356-022-21300-z

RESEARCH ARTICLE

Chemical characterization of water-soluble ions in highly time-resolved atmospheric fine particles in Istanbul megacity

Elif Mertoglu[1] · Hanny Dwiyari Amantha[1] · Rosa Maria Flores-Rangel[1]

Received: 5 January 2022 / Accepted: 1 June 2022 / Published online: 7 June 2022

Abstract

The diurnal and seasonal variations of water-soluble ions (WSIs) in fine particles were investigated in an area predominantly affected by traffic emissions in Beşiktaş, Istanbul between 2017 and 2018. $PM_{2.5}$ samples were collected at high time resolutions of 2 h during the daytime and 12 h during the nighttime for six sampling campaigns over all seasons. Five inorganic water-soluble ions (SO_4^{2-}, NH_4^+, NO_3^-, PO_4^{-3}, and NO_2^-) were determined using ion chromatography. Source analysis was investigated with principal component analysis (PCA) and bivariate polar plots. In descending order, WSIs concentrations were SO_4^{2-}>NH_4^+> NO_3^-> PO_4^{-3}>NO_2^- during the different seasons. The high time-resolved concentrations ranged as follows: sulfate 1.2–1118.1, ammonium 0.3–289.9, phosphate 2.9–107.6, nitrate 4.6–179.7, and nitrite 0.8–9.0 ng/m^3, with yearly averages of 226.5, 59.0, 58.4, 37.9, and 3.3 ng/m^3, respectively. Except for phosphate, all WSIs had strong seasonal variations with high concentrations during the winter and low concentrations during the summer. Molar ratios revealed that the formation of ammonium sulfate was less likely than ammonium nitrate. Principal component analysis resolved secondary aerosols (43.9%), residential heating (34.6%), shipping emissions (8.7%), and vehicle emissions (6.7%) as the major sources of WSIs, OC, EC, and $PM_{2.5}$ in Beşiktaş, Istanbul. Sulfate aerosol originated mainly from two nearby areas, SW and NE, of the sampling site tentatively due to residential heating and shipping emissions, respectively.

Keywords Water-soluble ions · Nitrate · Sulfate · Ammonium · Principal component analysis · Polar plots

Introduction

Atmospheric aerosols consisting of solid and liquid particles can be released from man-made or biogenic sources into the atmosphere (Begam et al. 2017). The primary inorganic aerosols such as Al, Fe, Mg, Ca, and Cl arise from natural, seawater, and man-made sources whereas secondary inorganic aerosols such as sulfate, nitrate, and ammonium can be derived from neutralization reactions (Shon et al. 2012). Aerosols can change the properties of the clouds by acting as cloud condensation nuclei and can absorb and scatter incident solar radiation (Venkataraman et al. 1999). Aerosols may also have serious effects on the decrease of visibility and air quality in the atmosphere and the impairment of human health (Shon et al. 2012). The diameter of the particles varies depending on their origin and the reactions they undergo in the atmosphere (Canepari et al. 2019). Fine particles having diameters smaller than 2.5 μm ($PM_{2.5}$) mainly originate from traffic emissions and production activities such as electricity or they can be derived from the process of gas-to-particle conversion in the atmosphere (Chakraborty and Gupta 2010). In particular, studies conducted in urban areas have shown that traffic emissions represent a significant source of secondary aerosols (Custodio et al. 2016). The chemical composition of $PM_{2.5}$ is varied (Ye et al. 2017), and the predominant species are secondary inorganic aerosols consisting of sulfate, nitrate, and ammonium in $PM_{2.5}$ (Dao et al. 2014; Lin 2002; Zhao et al. 2015). The formation of these ions is directly related to the precursor gases (He et al. 2018). The main pathway to produce sulfate is the oxidation of SO_2 which is mainly obtained from fossil fuel combustion. Sulfate can be also formed by ammonium sulfate ($(NH_4)_2SO_4$) and ammonium bisulfate (NH_4HSO_4), where these ammonium salts consist of a reaction between ammonia (NH_3) and sulfuric acid (H_2SO_4) (Bozkurt 2018).

Responsible Editor: Gerhard Lammel

✉ Rosa Maria Flores-Rangel
rflores@marmara.edu.tr

[1] Environmental Engineering Department, Marmara University Maltepe Campus, 34840 Istanbul, Turkey

The oxidation of NO_x and ammonium nitrate particles, which is formed by the reaction of nitric acid and ammonia, is the production pathway of nitrate (Shon et al. 2012). These water-soluble inorganic ionic species can exacerbate visibility impairment and affect the acidic (Gao et al. 2011) and hygroscopic properties of aerosols (Shen et al. 2009). It is necessary to determine their composition to better understand the environmental effects, properties, and reactivity of these ionic species (Deshmukh et al. 2010).

Istanbul is one of the second-largest metropolitan areas in the East Mediterranean with a population of over 15 million. Most of the pollution sources are derived from intense traffic and industry so that urbanization areas experience poor air quality levels (Krzyzanowski et al. 2014). According to Kanakidou et al. (2011), air quality limits of ozone and aerosol are often exceeded in the East Mediterranean. Poor quality coal used for residential heating caused the particulate matter (PM) and sulfur dioxide (SO_2) concentrations to exceed the air quality standard in Istanbul (Im et al. 2010). The climate of Istanbul is highly influenced by the proximity of the city to the sea and shows a transition between the Mediterranean and the Black Sea climate (Karaca et al. 1995).

In this work, high time-resolution $PM_{2.5}$ samples were collected to better understand the exchange of secondary water-soluble ions in the atmosphere and to interpret their possible sources. Firstly, the seasonal and diurnal variations of water-soluble ions were shown, and their relationship with meteorological factors was analyzed. Organic and elemental carbon together with water-soluble ions makes up the majority of fine particles (Ahmad et al. 2020). OC and EC concentrations reported by Flores et al. (2020a) and water-soluble ions were used in principal component analysis (PCA) in order to investigate their potential sources. This study is the first with its high sampling number and high time resolution covering four seasons for secondary water-soluble ions in Istanbul. This study on secondary ions is important in terms of helping to evaluate their adverse effects on humans and the atmosphere, as well as determining sources in a large metropolitan area such as Istanbul, especially in an area with high traffic.

Materials and methods

Study area and sampling site

Istanbul is the central city of Turkey and a highly populated megacity with a population of 15.52 million and an area of 5313 km^2. Diurnal measurements of fine particulate matter ($PM_{2.5}$) were carried out in the Beşiktaş district. The sampling station (41.0464 N, 29.0079 E) is on Barbaros Boulevard approximately 600 m North of the Bosphorus strait (Fig. 1). Istanbul is affected by various natural and anthropogenic emission sources. The sampling site is the receptor of road traffic and shipping emissions, the usage of poor quality coal for domestic heating during the heating season, and industrial activities in some parts of Istanbul. This area is also affected by airfield emissions.

Sample collection

Approximately 300 highly time-resolved $PM_{2.5}$ samples were collected on 8 × 10 in^2 quartz fiber filters (part number TE-QMA, Tisch Environmental, OH, USA) on selected days from January 2017 to January 2018 using a Tisch PNY-1123 high volume sampler. Samples were collected during the daytime with 2-h intervals between 7:00 and 19:00 and during the nighttime with 12-h intervals between 19:00 and 7:00. To investigate the influence of seasonal variations due to meteorology, samples were collected on selected periods as follows: Winter 1 (28/01/2017–04/02/2017), Winter 2 (17/02/2017–23/02/2017), Spring (03/05/2017–09/05/2017), Summer (06/07/2017–12/07/2017), Fall (20/10/2017–26/10/2017), and Winter 3 (05/01/2018–11/01/2018). Additional details about sampling preparation, collection, and instrument operation can be found elsewhere (Flores et al. 2020a).

Water-soluble ion analysis

Portions of $PM_{2.5}$ filter samples were placed in clean 50-ml polypropylene (pp) conical tubes with 10 ml ultrapure deionized water. The tubes were subjected to ultrasonic extraction for 60 min then centrifuged for 4 min at 2000 rpm. The extracted solutions were filtered with 0.22-µm microporous PTFE membranes. Finally, the filtered samples were transferred to 2-ml pp vials and stored at −4 °C until chemical analysis. A Shimadzu Prominence ion chromatography (IC) analyzer (HIC-20a Super) was used to determine the concentrations of anions (NO_2^-, NO_3^-, SO_4^{-2}, PO_4^{-3}) and a cation (NH_4^+). Calibration curves were performed for each working day, and blanks (deionized water) were analyzed every 10 samples to evaluate possible carryover from previous samples. Contamination from previous samples was not observed for any of the blank analyses.

Principal component analysis (PCA)

The potential sources of water-soluble ion species were evaluated by principal component analysis (PCA) (Hopke 2003). The purpose of PCA is to reduce the variables into a smaller number of components. The total contributions from various factors (i.e., sources) represent the measured concentration of the ion species at the receptor site (Ahmad et al. 2020). Contrary to other source analysis methods, in PCA, detailed knowledge of the sources is not required, and related studies about this can be widely found in the literature (Wei et al. 2019). In this study, OriginPro 2018 v.9.5.1.195 (OriginLab Co., Northampton, MA, USA) was used to carry out multivariate

Fig. 1 Study area and location of the sampling station

analysis via PCA. The input to the PCA was a 294 × 7 matrix with highly time-resolved concentrations of WSI determined in this study, and $PM_{2.5}$, organic carbon (OC), and elemental carbon (EC) concentrations reported by Flores et al. (2020a).

Meteorology and traffic data

Temperature (°C), dew point (°C), humidity (%), wind direction, wind speed (km h^{-1}), pressure (hPa),

precipitation (mm), and solar radiation (W m^{-2}) were obtained from Weather Underground at the closest meteorological station (i.e., Balmumcu, 41.0580 N, 29.0169 E) located 1570 m NE of the sampling station. Traffic density (number of vehicles per unit time) was obtained from the department of transportation in Istanbul for a sensor located nearly 460 m from the sampling site. Traffic data was not available for spring and summer sampling campaigns.

Results and discussion

Comparison of the WSIs with other studies in the world

The WSI concentrations obtained in this study were compared with other studies in the world. All studies were performed in urban areas with the exception of Tutsak and Koçak (2019) who performed the study in a rural (i.e., agricultural) area. The studies were selected based on geographical distribution and availability of seasonal concentrations in the fine fraction ($PM_{2.5}$). The seasonal and annual average concentrations are shown in Table 1. Overall, the highest concentrations among all selected studies were found in Jinan and Wuhan China (Gao et al. 2011; Zhang et al. 2022) and Delhi India (Jain et al. 2020) and were followed by a study in Seoul Korea (Lee et al. 2021). The lowest concentrations were observed in the urban traffic sites selected in this study: Erdemli Turkey (Tutsak and Kocak 2019), Oporto Portugal (Custódio et al. 2016), and Paris France (Bressi et al. 2013).

The seasonal average concentrations of nitrate, sulfate, and ammonium found by Gao et al. (2011) in Jinan were in the range of 10190–21770 ng/m^3, 27110–64270 ng/m^3, and 13280–29190 ng/m^3, respectively. These high concentrations were attributed to a combination of local emission sources such as traffic and residential heating and regional transport. Seasonal average concentrations in Wuhan

Table 1 Nitrate, sulfate, and ammonium concentrations (ng/m^3) in this study and in other urban and rural areas in the world

Region	Site	Season	NO_3^-	SO_4^{2}	NH_4^+	PO_4^{3-}	Reference
Istanbul, Turkey 2017–2018	Urban	Winter	42.12	227.83	75.70	37.33	This study
		Spring	11.47	103.22	16.46	32.10	
		Summer	37.10	263.79	84.08	25.28	
		Fall	50.70	265.88	83.26	35.43	
		Annual	34.94	219.25	64.07	34.61	
Erdemli, Turkey 2015	Rural	Winter	517	648	459	-	(Tutsak and Kocak 2019)
		Summer	256	1224	1715	-	
Jinan, China 2007–2008	Urban	Winter	21770	42840	29,190	-	(Gao et al. 2011)
		Spring	10190	27110	13280	-	
		Summer	19220	64270	28010		
		Fall	11690	30990	15130	-	
Wuhan, China 2014–2015	Urban	Winter	23210	14080	7440	-	(Zhang et al. 2022)
		Spring	7800	18070	5300	-	
		Summer	1130	14530	4830	-	
		Fall	15180	12870	7960	-	
Paris, France 2009–2010	Urban	Annual	2900	2000	1400	-	(Bressi et al. 2013)
Oporto, Portugal 2013–2014	Urban	Winter	1550	1090	560		(Custódio et al. 2016)
		Spring	840	1850	530		
		Summer	860	3330	890		
		Fall	1240	1690	480		
		Annual	1140	1950	620		
Seoul, Korea 2012–2013	Urban	Winter	11900	9300	6800		(Lee et al. 2021)
		Spring	10300	7800	5500		
		Summer	800	6800	2700		
		Fall	3800	4500	2200		
Delhi, India 2013–2016	Urban	Winter	20200	18600	16600		(Jain et al. 2020)
		Spring	6450	10400	6710		
		Summer	3500	9790	3020		
		Fall	18400	18100	14900		

(Zhang et al. 2022) were in the range of 1130–23210 ng/m^3 (nitrate), 12870–18070 ng/m^3 (sulfate), and 4830–7960 ng/m^3 (ammonium) and were also attributed to a combination of local emission sources (i.e., industrial emissions, coal combustion, vehicle emissions, and fugitive dust) as well as regional and long-range transport. The high concentrations of 3500–20200 ng/m^3 (nitrate), 9790–18600 ng/m^3 (sulfate), and 3020–16600 ng/m^3 (ammonium) reported by Jain et al. (2020) were mainly attributed to local sources such as biomass burning and traffic emissions, as well as transboundary sources for sulfate aerosol. The lower concentrations found in this work (i.e., nitrate 34.9 ng/m^3, sulfate 219.2 ng/m^3, and ammonium 64 ng/m^3) compared to other urban areas in the world may be attributed to the location of the sampling station away from industrial and residential areas contributing to residential heating emissions during the winter as will be explained in the following sections. Different seasonal variations were observed for different ion species in the selected studies. In our work, we found higher concentrations in the fall and winter and lower concentrations in the spring and summer for all target analytes. Similar results were obtained by Lee et al. (2021), Jain et al. (2020), and Zhang et al. (2022). In general, high concentrations in the winter have been attributed to an increase in emission sources such as biomass burning for residential heating during the cold season and traffic emissions, whereas high concentrations in the summer are due to an increase in the photochemical production of secondary inorganic aerosol.

Seasonal variation of WSIs

Figure 2 shows the fractional composition of water-soluble ions in $PM_{2.5}$ during the different seasons. Overall, the most abundant ion was sulfate with approximately 59 and 67% in the winter and spring, respectively. The second most abundant ion was variable. Both ammonium and phosphate contributed to approximately 20% of the investigated ions in the winter-fall and summer, respectively. The least abundant ions were nitrate and nitrite. Nitrate showed variations of approximately 7–11% in the summer and winter, respectively. While nitrite had abundances of 0.2–0.4% throughout all seasons.

The seasonal variation of water-soluble ions in $PM_{2.5}$ is shown in Fig. 3. In descending order, the concentrations are SO_4^{2-}> NH_4^+> NO_3^-> PO_4^{-3}> NO_2^-. The average seasonal concentrations ranged as follows: sulfate 103.22–265.88 ng/m^3, ammonium 16.46–87.67 ng/m^3, nitrate 11.47–50.70 ng/m^3, phosphate 25.28–39.38 ng/m^3, and nitrite 0.66–2.02 ng/m^3. Overall, two types of seasonal trends can be observed among the target compounds. Nitrite, nitrate, and phosphate show a decreasing trend from winter 1 to summer or fall, followed by an increasing trend in winter 3. On the other hand, sulfate and ammonium show an increasing trend from winter 1 to spring, and fall to winter, with lower concentrations in the summer.

All of the water-soluble ions measured in fine particles, with the exception of phosphate, were detected at the lowest concentrations in the summer. Sulfate was the most

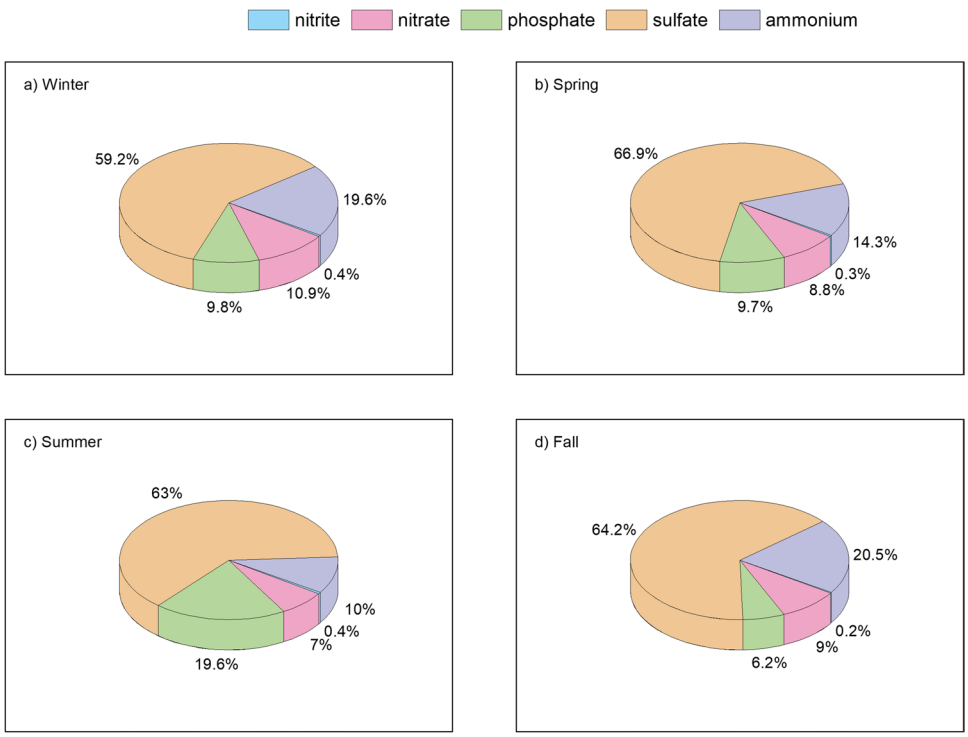

Fig. 2 Fractional composition of WSIs in $PM_{2.5}$ during different seasons

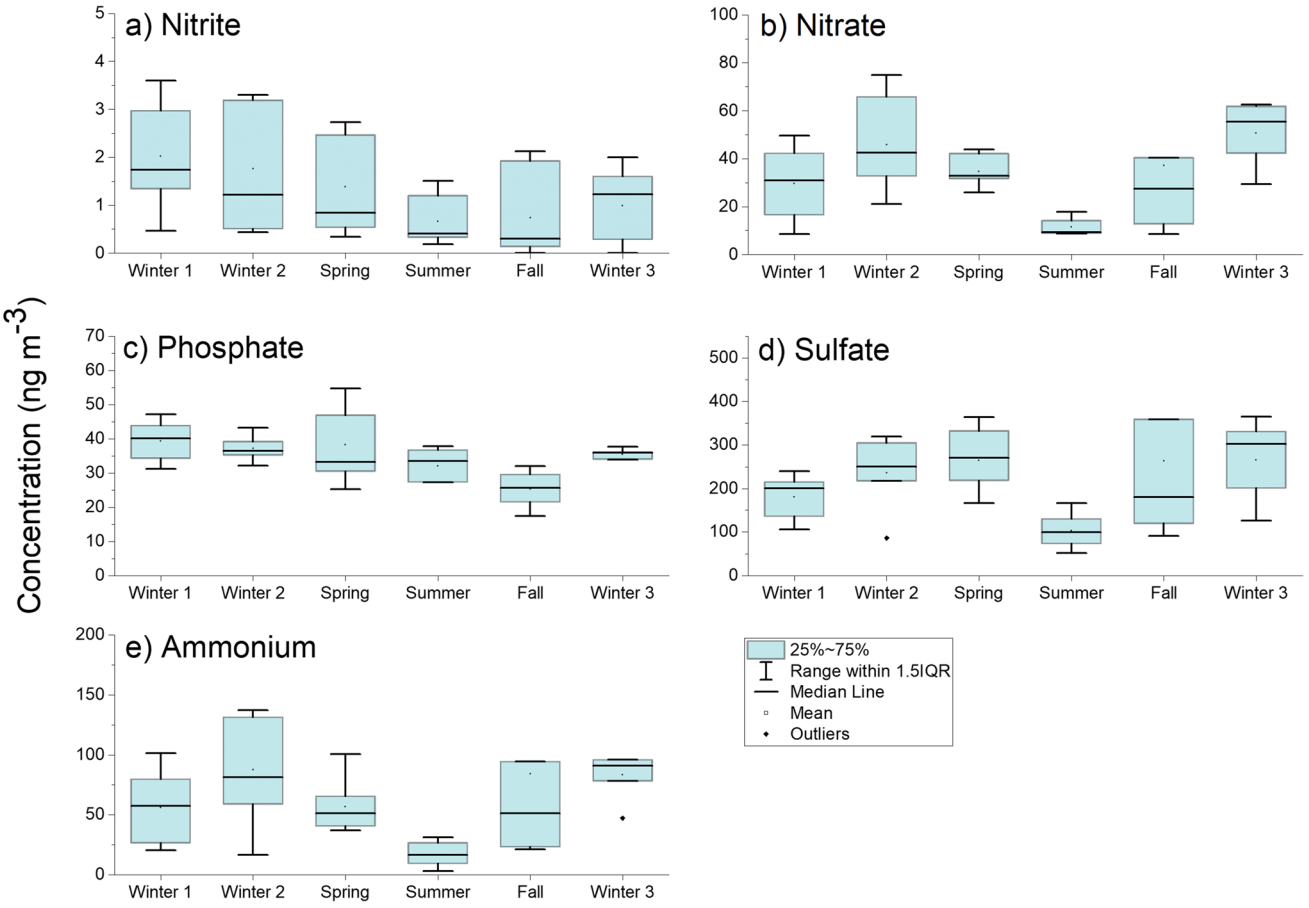

Fig. 3 Seasonal variation of WSIs

abundant ion in fine particles, accounting for approximately 60% of the total ions. Both SO_4^{2-} and NO_3^- secondary ions showed the highest concentrations during winter 3. It was observed that the changes in ammonium concentrations correspond to nitrate concentrations in three sampling periods (spring>winter 1>summer) while the sulfate concentrations in two sampling periods (winter 1>summer).

During the sampling periods, the total sulfate concentration appears to be approximately 3–4 times higher than the ammonium concentration, which has the highest concentration after sulfate. The high concentration of sulfate can be attributed to a high oxidation rate of sulfur dioxide (Lai et al. 2007). The decrease in ambient temperature, lower atmospheric deposition rates, increase in emissions from residential heating, and gas-to-particle conversion in the cold season may be associated with the accumulation of sulfate in the atmosphere and these high concentrations (Gao et al. 2011; Gao et al. 2019; Javed et al. 2015; Tutsak and Kocak 2019). In this work, it was observed that the sulfate concentration reaches high levels not only in the winter but also in the spring and fall seasons, which can be explained by the increasing sulfur dioxide conversion rates with increasing temperature and relative humidity (Jiang et al. 2018). In addition, the contribution of traffic emission to sulfate in $PM_{2.5}$ plays also a role in the high concentration levels (Zhao et al. 2011). Ammonia reacts with acidic gases in the atmosphere to form ammonium salts. Ammonium sulfate is the most common in the air because it is more stable than others. Ammonium nitrate exists in the atmosphere as a particulate form of nitrate although it is not stable enough (Lai et al. 2007). In high-temperature conditions, ammonium nitrate can decompose to nitric acid and ammonia (Javed et al. 2015; Tsai et al. 2016). Nitrite (NO_2^-), which originates from fossil fuel combustion, can be also transformed into nitrate particles by photo-oxidation reactions. The seasonal average concentrations of phosphate in decreasing order are winter 1 (39.38 ng/m^3), spring (38.26 ng/m^3), winter 2 (37.19 ng/m^3), winter 3 (35.43 ng/m^3), summer (32.10 ng/m^3), and fall (25.28 ng/m^3). The sources of phosphate have been reported in the literature as agricultural activities and the use of fertilizer (Bozkurt 2018; Chakraborty and Gupta 2010; Tsai et al. 2015); however, other sources include biomass burning, fossil fuel combustion, vehicle emissions, and mineral dust (Indris et al. 2020; Shi et al. 2019). The absence

of large variations during the different seasons may indicate that phosphate is emitted continuously from the same source during all seasons. Nitrite is not discussed in further sections due to its low concentrations compared to other ions.

Diurnal variation of WSIs

In order to understand the diurnal variation of WSIs, high time-resolved $PM_{2.5}$ samples were collected during different seasons at time resolutions of 2 h between 7:00 and 19:00 and 12 h during the nighttime (19:00–07:00). The average 2-h and 12-h concentrations are shown in Fig. 4 and are discussed according to each season. Figure 5 shows the time series of high time-resolved WSI concentrations (ng/m^3) in 2-h and 12-h $PM_{2.5}$ samples.

Winter

For all winter sampling campaigns (i.e., winter 1, winter 2, and winter 3), the lowest sulfate concentration was observed in the morning hours between 7:00 and 9:00. A gradual increase in the sulfate concentrations was observed from 07:00–09:00 to 15:00–17:00, possibly indicating a more predominant contribution of traffic emissions in this traffic sampling site. The maximum concentrations were observed at 15:00–17:00 and 13:00–15:00 in winters 1–2 and winter 3, respectively, which is consistent with diurnal patterns of traffic in this sampling site (Fig. 5a, (Flores et al. 2020a)). Higher concentrations during the daytime may be also explained by enhanced photochemical reactions due to stronger solar radiation (i.e., Fig 5c, (Flores et al. 2020a)). Overall, sulfate concentrations during the winter nighttime (19:00–07:00) were higher than early in the morning (i.e., 7:00–09:00), which may indicate the accumulation of pollutants with decreasing boundary layer height during this period (Gao et al. 2011). Contrary to sulfate, nitrate concentrations did not show strong diurnal variations. The low traffic density observed in the first hours of the morning may be the reason for the lower nitrate concentration during the 07:00–09:00 time interval in winter 1–3 sampling campaigns

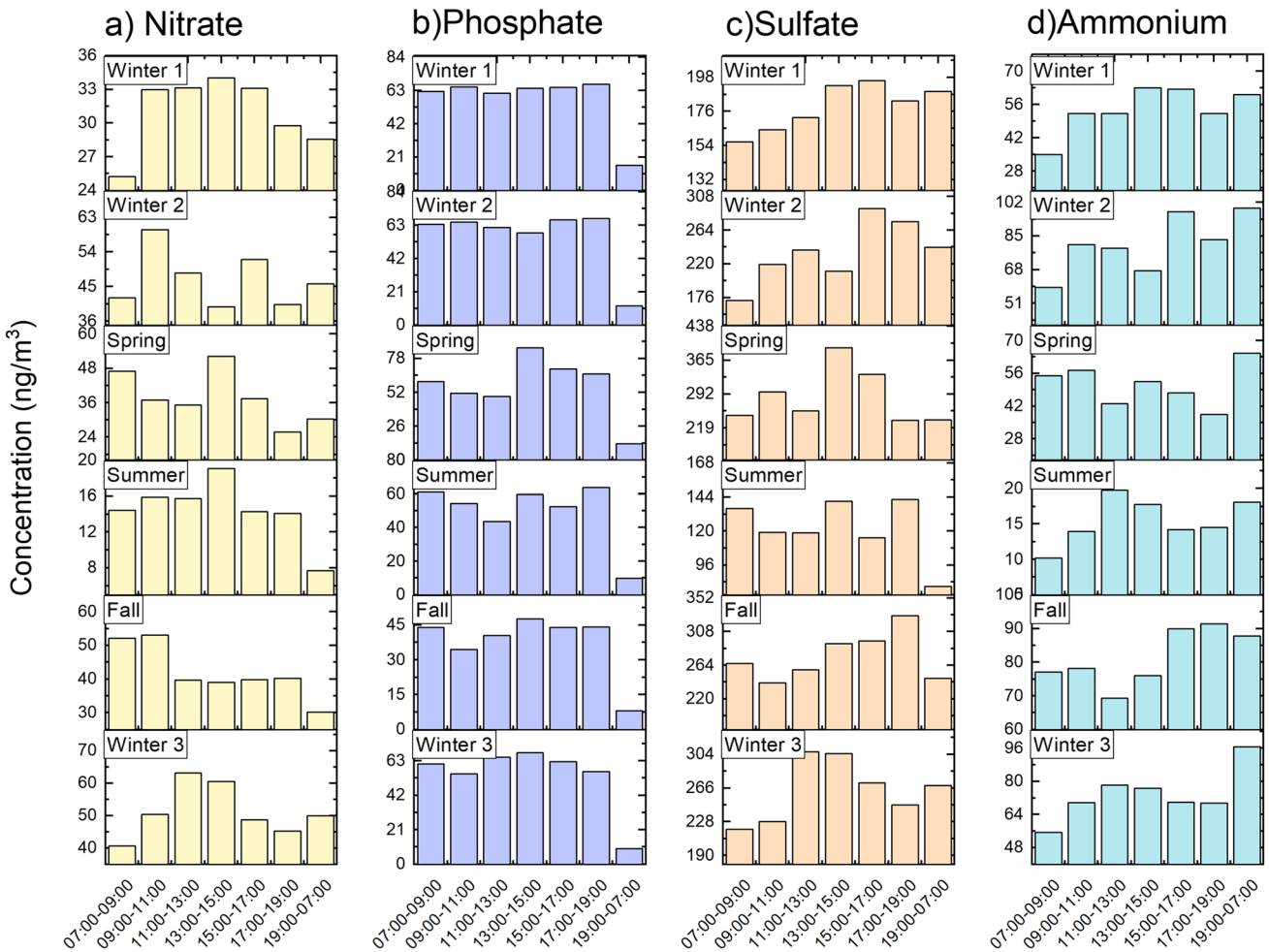

Fig. 4 Diurnal variability of water-soluble ion concentrations during the various sampling campaigns

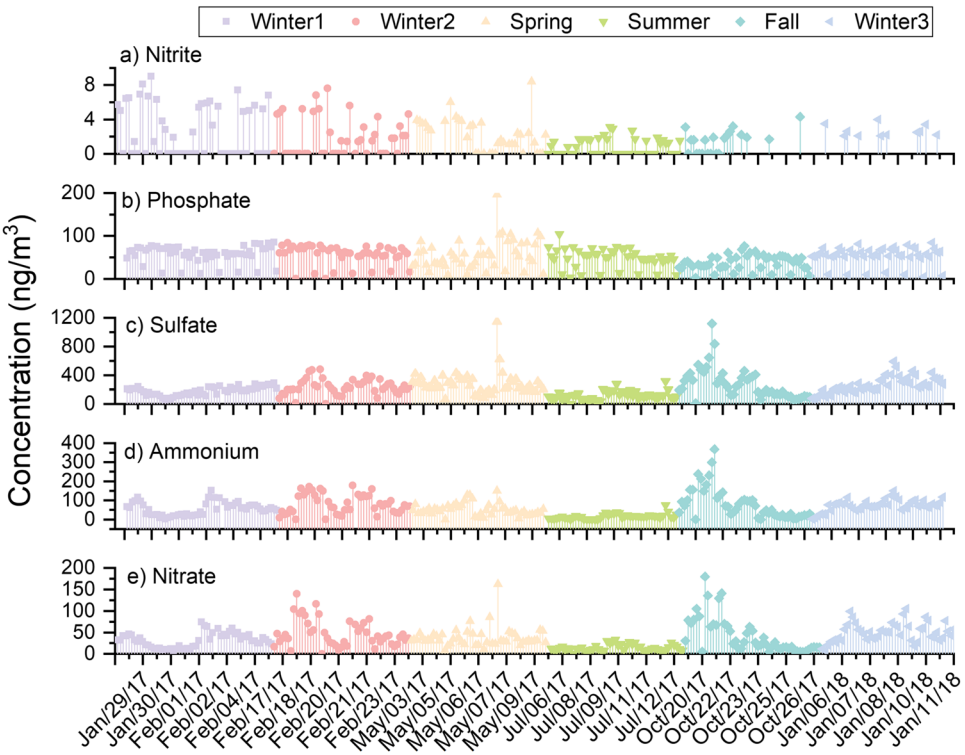

Fig. 5 Highly time-resolved concentrations of water-soluble ions in Istanbul

(Fig. 5a, (Flores et al. 2020a)). The nitrate concentrations did not change significantly during the daytime by maintaining the thermodynamic balance with the decreasing temperatures in the winter period (Gao et al. 2011). Ammonium concentrations varied in the range of 35.05–62.66, 59.09–99.03, and 55.32–96.64 ng/m^3 in winter 1–3 sampling campaigns, respectively (Fig. 4d). Ammonium concentrations steadily increased during the day and reached the maximum concentrations during the nighttime. The reasons for this may be connected with an increase in relative humidity and accumulation of particles by a decrease in the boundary layer height (Tutsak and Kocak 2019). The phosphate concentration did not show any significant diurnal pattern in all winter periods; however, concentrations were much lower during the nighttime (i.e., 9.50–15.79 ng/m^3) than in the daytime (i.e., 61.04–63.72 ng/m^3). This may be an indicator of a decrease in transport from local or regional sources during the nighttime.

Spring

The maximum concentrations of sulfate were observed in the spring at 13:00–15:00 and 15:00–17:00 (Fig. 4c). Although traffic density data was not available during the spring, the maximum sulfate concentrations coincide with the diurnal traffic patterns in other seasons as shown by Flores et al. (2020a). In addition, meteorological conditions such as low boundary layer height and high temperature (Fig. 6) may have contributed to the enhanced production of sulfate particles during the spring compared to other seasons. The diurnal variation of nitrate and phosphate exhibited similarity with sulfate, with maximum and minimum concentrations at the same time intervals. Similar variations among these three secondary ions may indicate similar sources in the spring season.

Summer

Contrary to the cold season, sulfate reached its lowest concentration during the nighttime (19:00–07:00) in the warm season. The decline in the photochemical reactions due to the lack of solar radiation and the effect of prevailing northerly winds (N, NNE, and ENE) may be the reason for the lower concentrations during the nighttime. The dilution of pollutants owing to boundary layer height in the warm season may also influence the decreased concentrations during the nighttime. The maximum sulfate concentration was observed at 17:00–19:00 which was similar to the early morning period (07:00–09:00). High concentration values at 07:00–09:00 can be explained by poor atmospheric dilution due to very low boundary layer heights (Fig. 6). Although the boundary layer height increased at 17:00–19:00 and the wind speed reached its highest value (4.99 m/s), sulfate showed a high concentration during this period, which may indicate the influence of atmospheric transport from nearby regions. Ammonium and nitrate concentrations showed a

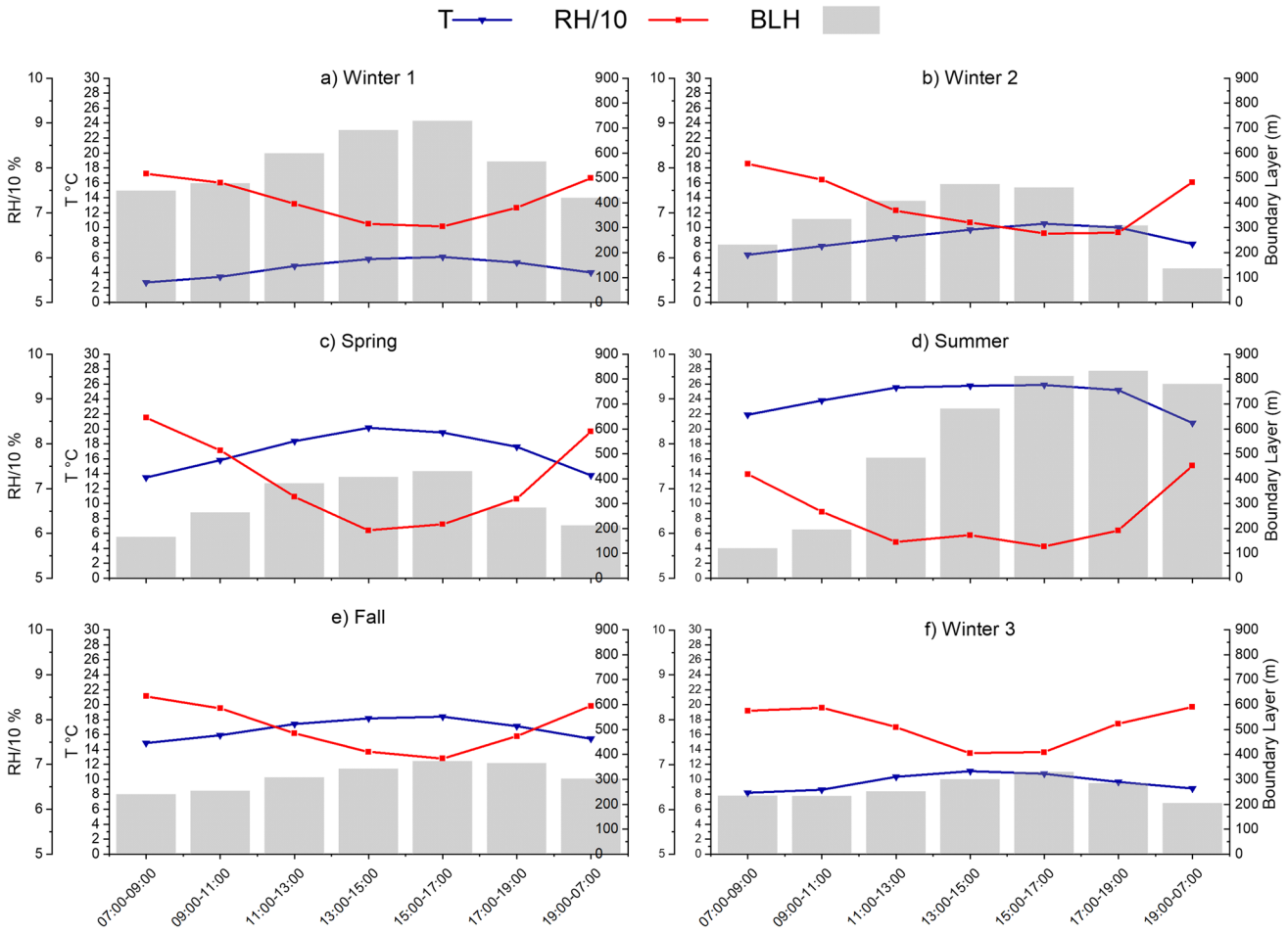

Fig. 6 Diurnal variability of temperature, relative humidity, and boundary layer height during the various sampling campaigns

similar trend except for the nighttime period. Nitrate was measured at its minimum concentration in the nighttime (7.70 ng/m^3) while ammonium concentration showed a slight increase in the concentration (18.10 ng/m^3) compared to the daytime. The reason for lower nitrate concentration during the summer may be attributed to the decomposition of NH_4NO_3 under the effect of higher temperatures (Gao et al. 2011). On the other hand, an increase in the ammonium concentration during the nighttime may be due to variations in meteorological conditions. Phosphate concentrations did not show significant variation during the daytime; however, the concentrations significantly decreased during the nighttime possibly due to reduced transport from local emissions.

Fall

The maximum concentration of sulfate (328.70 ng/m^3) was observed at 17:00–19:00. Contrary to spring and summer, sulfate concentration was found at low levels at 9:00–11:00, rising slowly until 19:00 and decreasing during the nighttime. The lack of a sharp increase in the concentrations during the daytime may be due to lower solar radiation during the fall, compared to spring and summer. Nitrate (52.99 ng/m^3) and ammonium (91.36 ng/m^3) concentrations peaked at 09:00–11:00 and 17:00–19:00 time intervals, respectively. Unlike other seasons, it was observed that sulfate, nitrate, and ammonium were at a high concentration in the fall season between 7:00 and 09:00, which may be due to a combination of low boundary layer height and wind speed.

The molar ratios between ionic species can be used as a first analysis to understand variations of emission sources and processes involved in the formation of secondary inorganic aerosol. Table 2 shows the diurnal and seasonal variation of molar ratios SO_4^{2-}/NO_3^-, NH_4^+/NO_3^-, and NH_4^+/SO_4^{2-}.

The average values of SO_4^{2-}/NO_3^- ratios ranged from 5.5 to 9.4 during the different seasons. Similar average ratios were observed in the spring (7.7) and fall (7.4) whereas significant variations were observed in the winter and summer, with lower ratios in the winter (5.5) and higher ratios in the summer (9.4). Although a dramatic decrease in the concentrations was observed for both sulfate and nitrate

aerosol during the summer, in addition to traffic emissions, high concentrations of sulfate aerosol are also due to shipping emissions near the sampling site. The diurnal values of SO_4^{2-}/NO_3^- ratios ranged 4.4–6.1, 5.3–9.1, 7.4–10.5, and 4.6–8.2 in the winter, spring, summer, and fall, respectively, with lower ratios in the morning (07:00–11:00) and higher ratios in the late afternoon (17:00–19:00). This diurnal variation may indicate the predominance of local sources from traffic emissions in the morning and the transport of sulfate aerosol in the afternoon due to variations in the boundary layer height, particularly in the summer (Fig. 6). Higher ratios in the summer compared to the winter may also be due to variations in temperature that favor the formation of sulfate aerosol and degradation of nitrate aerosol during the summer (i.e., high temperature) and formation of nitrate aerosol during the winter (i.e., low temperature) (Jain et al. 2020).

The molar ratios NH_4^+/NO_3^- and NH_4^+/SO_4^{2-} are helpful to show the likely formation of ammonium nitrate $(NH_4)_2NO_3$ and ammonium sulfate $(NH_4)_2SO_4$, respectively, through neutralization reactions. Ratios greater than 1 and 2 indicate the presence of sufficient ammonium aerosol in the atmosphere to completely neutralize the nitrate and sulfate, respectively, and favor the formation of secondary inorganic aerosol. In this work, the molar ratios NH_4^+/NO_3^- were greater than 1 during all seasons and times of the day, with the exception of summer 09:00–11:00 and 13:00–15:00 which were 0.9 in both cases, indicating the formation of ammonium nitrate during most of the sampling campaigns. The ratios ranged as 1.4–2.1, 1.0–2.1, 0.9–2.4, and 1.5–2.9 in the winter, spring, summer, and fall, respectively with the highest ratios (2.1–2.9) in nighttime samples (19:00–07:00). High ratios observed during the nighttime may be likely due to the decrease in nitrate aerosol from traffic emissions (Fig. 4a). The molar ratios of NH_4^+/NO_3^- did not show significant seasonal variations in the winter, spring, and summer with values of 1.7–1.8. However, greater values were observed in the fall (2.4). These high ratios in the fall may be due to a decrease in the nitrate aerosol (Fig. 4a) and an increase of ammonium aerosol (Fig. 4d) available during the nighttime (i.e., ratio 2.9, 19:00–07:00, Table 2).

Contrary to NH_4^+/NO_3^- ratios, the formation of ammonium sulfate was less likely than ammonium nitrate since ratios of NH_4^+/SO_4^{2-} did not exceed the value of 2 estimated by thermodynamic models during the daytime and nighttime samples at all seasons. In addition, the ratios did not show strong diurnal and seasonal variations and were in the range of 0.1–0.4. One possible explanation is that sulfate aerosol and ammonia may be emitted by different sources and are present at different geographical locations inhibiting the formation of ammonium sulfate. Bivariate polar plots in further sections will show that nitrate and ammonium aerosols are present in high concentrations near the sampling site, while sulfate aerosol is transported from nearby areas in the SW direction (Fig. 7). Another possible explanation may be due to the presence of organic material in this urban traffic site, coating the aerosol and retarding the formation of ammonium sulfate as explained by Silvern et al. (2017).

Bivariate polar plots

Bivariate polar plots were used to identify potential sources of WSIs. Polar plots were created with the open-source package openair (Uria-Tellaetxe and Carslaw 2014) with high time-resolved concentrations (i.e., 2 h and 12 h averages) of $PM_{2.5}$ and WSI concentrations. Figure 7 shows the annual polar plots of $PM_{2.5}$ and WSIs. Polar plots identified various sources for $PM_{2.5}$ and water-soluble ions. In general, during the study period, northeast (NE) was the dominant wind direction with wind speeds as high as 8.5 m s^{-1}. Southwesterly (SW) and southeasterly (SE) winds were also observed with lower frequencies and wind speeds (i.e., 4 m s^{-1}). In this traffic site, high concentrations of $PM_{2.5}$ (Fig. 7a), nitrate (Fig. 7c), sulfate (Fig. 7e), and ammonium (Fig. 7f) were observed during stable conditions or episodes with wind speeds lower than 2 m s^{-1}. Transport from the SW direction resulted in high concentrations of nitrite (Fig. 7b),

Table 2 Molar ratios between sulfate, nitrate, and ammonium ions in $PM_{2.5}$

	SO_4^{2-}/NO_3^-				NH_4^+/NO_3^-				NH_4^+/SO_4^{2-}			
	Winter	Spring	Summer	Fall	Winter	Spring	Summer	Fall	Winter	Spring	Summer	Fall
07:00–09:00	5.2	5.3	9.4	5.1	1.4	1.2	0.7	1.5	0.3	0.2	0.1	0.3
09:00–11:00	4.4	8.0	7.5	4.6	1.4	1.6	0.9	1.5	0.3	0.2	0.1	0.3
11:00–13:00	5.0	7.3	7.5	6.5	1.5	1.2	1.3	1.7	0.3	0.2	0.2	0.3
13:00–15:00	5.3	7.5	7.4	7.5	1.6	1.0	0.9	1.9	0.3	0.1	0.1	0.3
15:00–17:00	5.7	8.9	8.1	7.4	1.7	1.3	1.0	2.3	0.3	0.1	0.1	0.3
17:00–19:00	6.1	9.1	10.1	8.2	1.8	1.5	1.0	2.3	0.3	0.2	0.1	0.3
19:00–07:00	5.8	7.8	10.5	8.2	2.1	2.1	2.4	2.9	0.4	0.3	0.2	0.4
Average	5.5	7.7	9.4	7.4	1.8	1.7	1.7	2.4	0.3	0.2	0.2	0.3

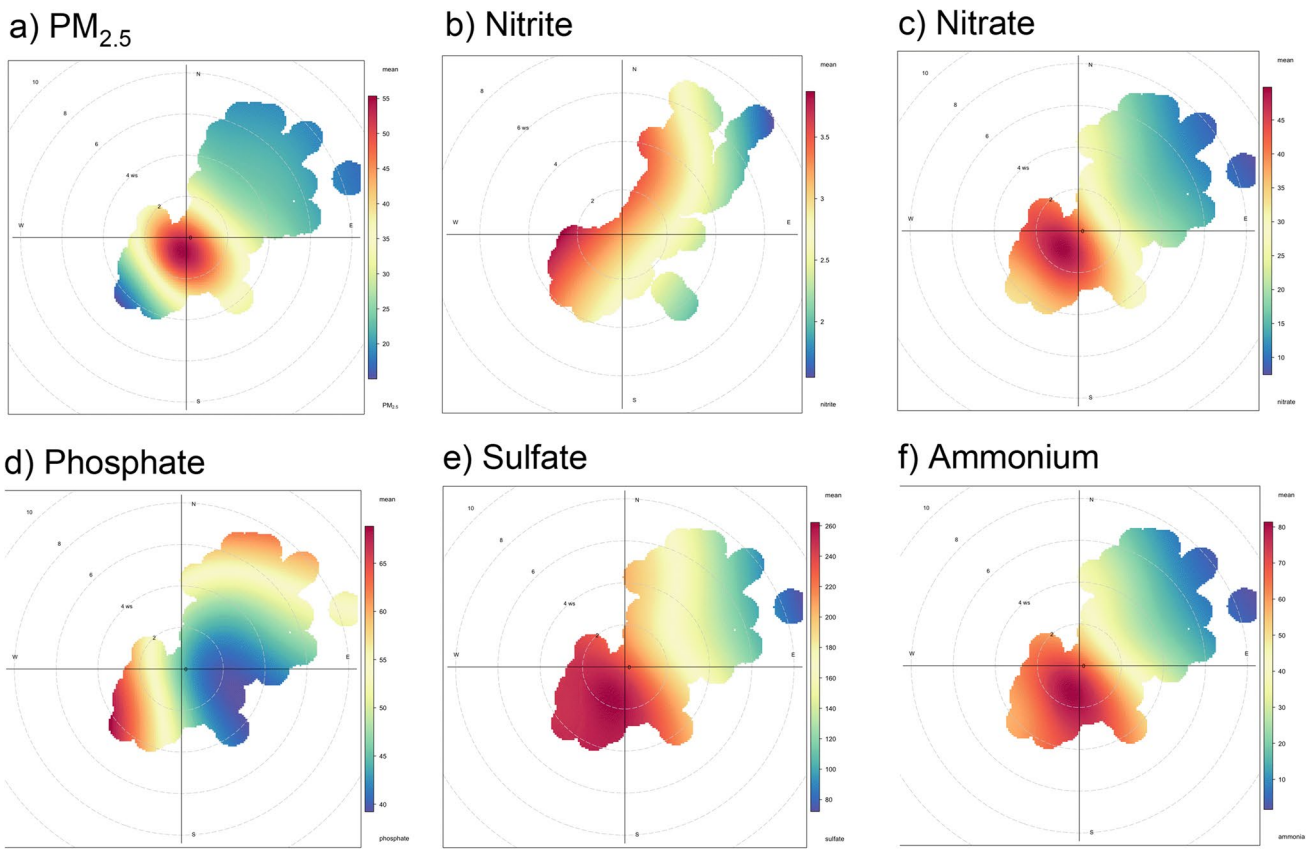

Fig. 7 Annual polar plots of highly time-resolved concentrations of (**a**) $PM_{2.5}$ and (**b**–**f**) water-soluble ions

phosphate (Fig. 7d), sulfate, and in lower quantities of nitrate and ammonium. A fraction of ammonium ion was also transported from the SE. An additional source identified NE of the sampling site was associated with lower concentrations of nitrite, phosphate, and sulfate ions. These results are consistent with previous studies that have identified sources such as traffic emissions near the sampling site at low wind speeds, shipping emissions from the NE and SE directions, and fossil fuel combustion from residential heating from the SW and SE directions (Baykara et al. 2019; Flores et al. 2020b; Flores et al. 2022; Şahin et al. 2020).

Source identification by principal component analysis (PCA)

Principal component analysis was performed with OriginPro 2018 v.9.5.1.195 (OriginLab Co., Northampton, MA, USA). The input matrix was composed of 300 highly time-resolved concentrations of nitrate, phosphate, sulfate, and ammonium ions. $PM_{2.5}$, OC, and EC concentrations (Flores et al. 2020a) were also used to aid in the identification of sources. Overall, four factors resolved 93.9% of the total variance of the data. Table 3 shows the extracted coefficients.

The results show that factors 1 and 2 had the highest contribution to the total variance of the data (78.5%), while factors 3 and 4 had a minor contribution (15.4%). Factor 1 had the highest contribution to the total variance of the data (43.9%) and was composed of nitrate, sulfate, ammonium, and $PM_{2.5}$ and was interpreted as secondary inorganic aerosol (Zhang et al. 2022). Factor 2 (34.6%) was composed of phosphate and sulfate, which showed negative correlations with OC and EC. In a previous study, OC and EC were associated with traffic emissions near the sampling site and shipping emissions from the NE and E directions, respectively (Flores et al. 2022). Source analysis performed with polar plots in "Bivariate polar plots" section identified sources of phosphate and sulfate from the SW, NE, as well as sources near the sampling site. Since phosphate and sulfate had negative correlations with OC and EC which were associated with sources near the sampling site and NE, respectively, factor 2 was interpreted as fossil fuel combustion from the SW direction, which is consistent with emissions from residential heating

Table 3 Extracted principal components and their loading coefficients

	Factor 1 Secondary aerosol	Factor 2 Residential heating	Factor 3 Shipping	Factor 4 Traffic
Nitrate	**0.47**	0.28	0.00	0.00
Phosphate	−0.11	**0.52**	0.29	**0.73**
Sulfate	**0.43**	**0.29**	**0.44**	−0.15
Ammonium	**0.52**	0.16	0.00	−0.32
OC	0.29	**−0.48**	0.25	**0.41**
EC	0.18	**−0.55**	**0.41**	0.09
$PM_{2.5}$	**0.43**	−0.10	**−0.71**	**0.40**
Eigenvalue	3.07	2.42	0.61	0.47
Percent variance	43.9	34.6	8.7	6.7
Cumulative variance	43.9	78.5	87.2	93.9

(Baykara et al. 2019). These observations are also consistent with polar plots performed for each winter campaign (Fig. 8).

Factors 3 and 4 had the lowest contribution to the total variance of the data with 8.7 and 6.7%, respectively. Factor 3 was composed of sulfate and EC and had a large negative correlation with $PM_{2.5}$ concentrations. Following the discussion in factor 2, factor 3 was interpreted as shipping emissions from the NE direction, as shown in Figs 7e and 8a, and due to the negative correlation with $PM_{2.5}$ concentrations emitted near the sampling site (Fig. 7a). Factor 4 (6.7%) had high contributions of phosphate, OC, and $PM_{2.5}$. Since $PM_{2.5}$ and OC concentrations have been associated with sources near the sampling site during calm conditions, this factor may be associated with sources of phosphate near the sampling site. Gasoline and motor lubricating oils contain phosphate-based additives in low quantities (Indris et al. 2020; Spencer et al. 2006). Although the source was not clearly identified by polar plots (Fig. 7d), factor 4 was interpreted as a source near the sampling site, tentatively named as traffic.

Correlation among WSIs, air pollutants, and meteorological factors

In this section, the relationship among WSIs, gas-phase air pollutants SO_2 and NO_2, and meteorological factors are determined by Pearson correlation analysis (Table 4). High correlation values indicate that the pollutants originate from the same source or are exposed to similar atmospheric

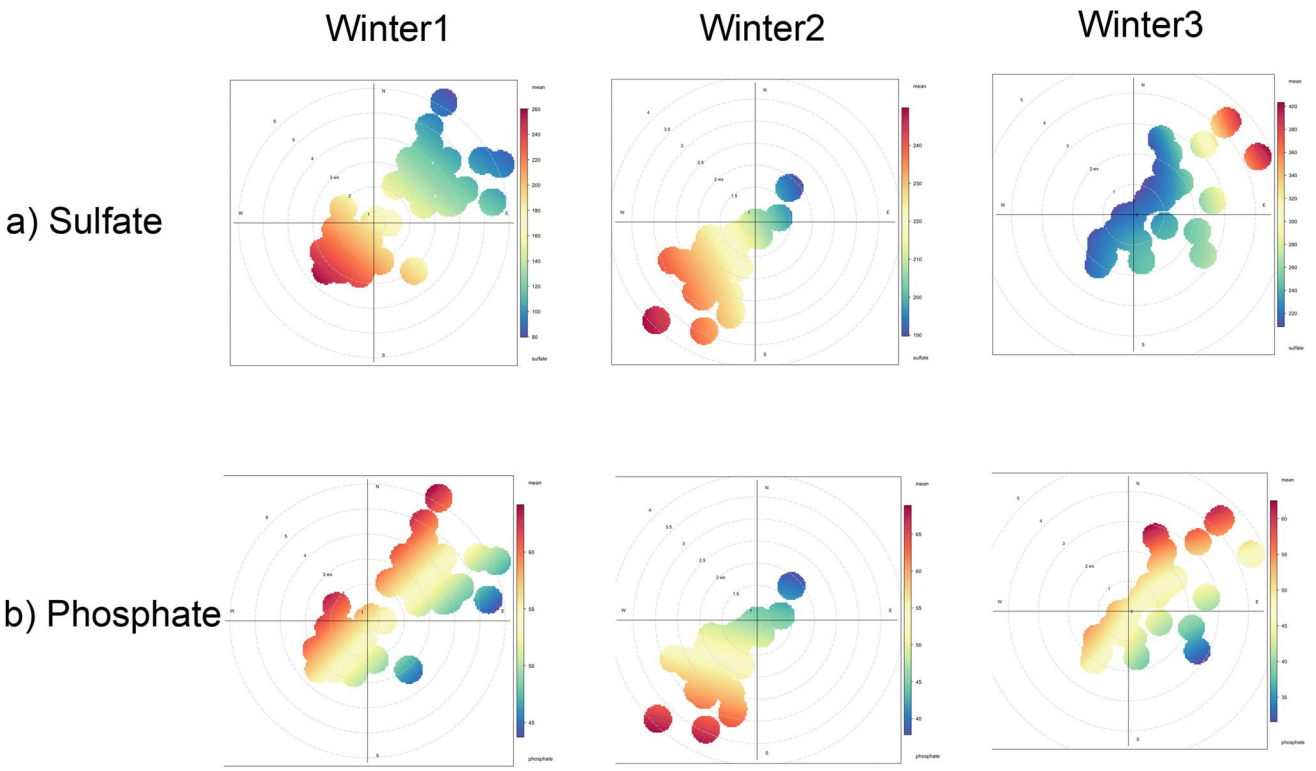

Fig. 8 Polar plots of highly time-resolved concentrations of (**a**) sulfate and (**b**) phosphate during winter 1 (left), winter 2 (middle), and winter 3 (right)

processes (Bozkurt 2018). It has been determined that all ionic compounds with the exception of phosphate and gas pollutants are moderately and strongly correlated with each other during winter 1. Secondary water-soluble ions have been transformed in the atmosphere under certain chemical reactions. Therefore, they have been exposed to similar conditions in the atmosphere (i.e., temperature and solar radiation). The formation of ammonium sulfate and bisulfate resulting from the reaction between sulfuric acid and ammonium can explain the strong correlation between ammonium and sulfate. During winter 2, the moderate and strong correlations between ammonium, nitrate, phosphate, and sulfate may indicate homologous anthropogenic sources (Zhang et al. 2019). Phosphate exhibited moderate and strong correlation with sulfate in winter 2 and winter 3, respectively. The correlation between phosphate and ammonium may indicate the formation of $(NH_4)_3PO_4$ from the reaction between H_3PO_4 and NH_3 in the atmosphere (Bozkurt 2018). Moderate and strong correlations were found between sulfate and nitrate ions with their gas-phase precursors SO_2 and NO_2, particularly during the winter and fall (Wang et al. 2006). Wind speed determines the transport of air pollutants, allowing them to dilute in the atmosphere. On the other hand, a positive effect between wind speed and air pollutants may be their transport to the receptor site after emission, thus, increasing their concentration in the atmosphere. It is seen

Table 4 Pearson correlation analysis

	NO_3^-	PO_4^-	SO_4^{2-}	NH_4^+	NO_3^-	PO_4^-	SO_4^{2-}	NH_4^+
Winter 1					**Summer**			
PO_4^-	0.14				−0.04			
SO_4^{2-}	**0.62**	0.45			0.24	**0.82**		
NH_4^+	**0.9**	0.4	**0.89**		**0.56**	**−0.6**	−0.2	
SO_2	0.27	**0.52**	**0.92**	**0.66**	0.31	−0.01	0.35	0.06
NO_2	**0.72**	0.01	**0.78**	**0.79**	−0.18	−0.1	−0.2	−0.5
T	**0.65**	0.36	**0.97**	**0.88**	0.32	−0.3	−0.2	**0.78**
RH	**−0.7**	−0.3	**−1**	**−0.9**	−0.23	0.45	0.3	**−0.8**
SR	**0.84**	−0.3	**0.6**	**0.76**	**0.72**	**−0.6**	−0.4	**0.86**
WS	**0.65**	0.17	**0.94**	**0.86**	0.19	0.06	0.08	0.49
P	−0.1	**−0.7**	**−0.8**	**−0.5**	0.24	−0.4	−0.3	−0
BLH	**0.67**	0.16	**0.95**	**0.87**	0.03	0.09	0.15	0.42
Winter 2					**Fall**			
PO_4^-	0.33				**−0.6**			
SO_4^{2-}	0.18	**0.54**			**−0.65**	**0.71**		
NH_4^+	**0.51**	**0.58**	**0.93**		−0.21	0.23	**0.74**	
SO_2	−0.4	−0.2	**0.67**	0.46	**−0.89**	0.43	**0.79**	0.48
NO_2	−0.4	0.47	**0.7**	0.44	−0.19	**−0.6**	−0	0.01
T	−0.2	0.09	**0.85**	**0.69**	**−0.91**	0.44	0.49	0.24
RH	0.25	−0.1	**−0.8**	**−0.6**	**0.91**	**−0.5**	**−0.6**	−0.4
SR	0.13	**−0.6**	0.26	0.29	−0.43	−0	−0.3	−0.6
WS	0.23	**−0.7**	0.02	0.12	**−0.81**	0.45	**0.71**	**0.65**
P	0.42	**−0.5**	**−0.7**	−0.5	0.08	**−0.5**	**−0.7**	**−0.9**
BLH	0.11	−0.4	0.46	0.46	**−0.9**	**0.55**	**0.81**	**0.59**
Spring					**Winter 3**			
PO_4^-	0.48				0.65			
SO_4^{2-}	**0.63**	**0.72**			**0.89**	**0.82**		
NH_4^+	**0.71**	0.01	0.39		**0.9**	0.42	**0.85**	
SO_2	**−0.5**	0.45	0.03	**−0.8**	−0.06	0.05	0.28	0.29
NO_2	−0.1	**−0.6**	**−0.5**	**0.53**	0.11	**−0.6**	−0.3	0.17
T	−0	**0.56**	**0.65**	−0.4	**0.68**	**0.7**	**0.91**	**0.78**
RH	0.08	**−0.6**	**−0.6**	**0.5**	−0.44	**−0.7**	**−0.7**	**−0.5**
SR	0.34	0.16	**0.65**	0.09	**0.96**	**0.77**	**0.91**	**0.83**
WS	−0.3	0.47	**0.49**	**−0.5**	**0.96**	**0.77**	**0.91**	**0.83**
P	0.42	**−0.6**	−0.2	**0.68**	**0.95**	**0.67**	**0.95**	**0.91**
BLH	0.02	0.41	**0.65**	−0.3	0.13	0.38	0.49	0.37

that wind speed has a positive relationship with secondary ions, during the different seasons, particularly during the winter and fall, which may indicate transport from nearby areas. Phosphate was negatively correlated with wind speed during winter 2, while no significant negative or positive correlation was found for other pollutants. Temperature had positive moderate and strong correlations with WSIs during the different seasons, except summer. High local temperatures create a favorable environment for the formation of secondary ions, particularly the conversion of nitrogen dioxide and sulfur dioxide to the particle phase (Hong et al. 2018). However, the unstable nature of nitrate causes its conversion to nitric acid in gaseous form under high temperatures (Wei et al. 2019). Relative humidity is inversely correlated with all pollutants.

Summary and conclusions

This study has yielded highly time-resolved concentrations of water-soluble ions SO_4^{2-}, NH_4^+, NO_3^-, PO_4^{-3}, and NO_2^- during six sampling campaigns and four seasons, in an area exposed to heavy traffic in Beşiktaş, Istanbul between 2017 and 2018. In descending order, the averaged seasonal concentrations of WSIs were SO_4^{2-}>NH_4^+> NO_3^-> PO_4^{-3}> NO_2^-, respectively. All of the water-soluble ions analyzed in $PM_{2.5}$, with the exception of phosphate, were observed at the lowest concentrations in the summer. Sulfate was the most abundant ion in fine particles, accounting for 59–67% of the total ion concentrations. During all sampling campaigns, sulfate concentrations were approximately 3–4 times higher than ammonium concentrations. The high concentrations of sulfate can be attributed to fossil fuel combustion from residential heating from the SW and to a lesser extent shipping emissions from the NE. The decrease in temperatures, lower atmospheric deposition, increase of emissions from residential heating, and minor gas to particle conversion rate in the winter months may be associated with the accumulation of sulfate in the atmosphere and these high concentrations. Sulfate also showed high concentrations in the spring and fall, which can be explained by the increasing sulfur dioxide conversion rates with increasing temperature and relative humidity. Nitrate did not show strong diurnal variations. Similarly, phosphate did not show significant diurnal patterns; however, concentrations were much lower during the nighttime. Principal component analysis resolved secondary aerosols (43.9%), residential heating (34.6%), shipping emissions (8.7%), and vehicle emissions (6.7%) as the major sources of WSIs, OC, EC, and $PM_{2.5}$ in Beşiktaş, Istanbul. A shortcoming of this work is the number of possible sources identified by the chemical species investigated in this study. Future work may consider expanding this study to a larger number of target compounds to identify additional sources such as biomass burning, industrial emissions, sea salt aerosol, and mineral dust.

Acknowledgements The authors would like to express their immense gratitude to Assoc. Prof. Bilge Alpaslan Kocamemi and Bugra Senol for their help with ion chromatography analysis.

Author contribution Elif Mertoglu: methodology, investigation, writing—original draft preparation. Hanny D. Amantha: methodology, investigation, writing—reviewing and editing. Rosa M. Flores: conceptualization, funding acquisition, supervision, writing—reviewing and editing.

Funding This work was partially supported by the Scientific and Technological Research Council of Turkey (TÜBITAK) through project No. 115Y625.

Data availability All data generated or analyzed during this study are included in this published article and its supplementary information files.

Declarations

Ethics approval Not applicable. This manuscript does not involve researching humans or animals.

Consent to participate All of the authors consented to participate in the drafting of this manuscript.

Competing interests The authors declare no competing interests.

References

Ahmad M, Cheng SM, Yu Q, Qin WH, Zhang YP, Chen J (2020) Chemical and source characterization of PM2.5 in summertime in severely polluted Lahore, Pakistan. Atmos Res 234:104715. https://doi.org/10.1016/j.atmosres.2019.104715

Baykara M, Im U, Unal A (2019) Evaluation of impact of residential heating on air quality of megacity Istanbul by CMAQ. Sci Total Environ 651:1688–1697. https://doi.org/10.1016/j.scitotenv.2018.10.091

Begam GR, Vachaspati CV, Ahammed YN, Kumar KR, Reddy RR, Sharma SK, Saxena M, Mandal TK (2017) Seasonal characteristics of water-soluble inorganic ions and carbonaceous aerosols in total suspended particulate matter at a rural semi-arid site, Kadapa (India). Environ Sci Pollut Res 24:1719–1734. https://doi.org/10.1007/s11356-016-7917-1

Bozkurt Z (2018) Seasonal variation of water-soluble inorganic ions in PM10 in a city of northwestern Turkey. Environ Forensic 19:1–13. https://doi.org/10.1080/15275922.2017.1408159

Bressi M, Sciare J, Ghersi V, Bonnaire N, Nicolas JB, Petit JE, Moukhtar S, Rosso A, Mihalopoulos N, Féron A (2013) A one-year comprehensive chemical characterisation of fine aerosol (PM_{2.5}) at urban, suburban and rural background sites in the region of Paris (France). Atmos Chem Phys 13:7825–7844. https://doi.org/10.5194/acp-13-7825-2013

Canepari S, Astolfi ML, Catrambone M, Frasca D, Marcoccia M, Marcovecchio F, Massimi L, Rantica E, Perrino C (2019) A combined chemical/size fractionation approach to study winter/summer variations, ageing and source strength of atmospheric particles.

Environ Pollut 253:19–28. https://doi.org/10.1016/j.envpol.2019.06.116
Chakraborty A, Gupta T (2010) Chemical characterization and source apportionment of submicron (PM1) aerosol in Kanpur Region, India. Aerosol Air Qual Res 10:433–445. https://doi.org/10.4209/aaqr.2009.11.0071
Custodio D, Cerqueira M, Alves C, Nunes T, Pio C, Esteves V, Frosini D, Lucarelli F, Querol X (2016) A one-year record of carbonaceous components and major ions in aerosols from an urban kerbside location in Oporto, Portugal. Sci Total Environ 562:822–833. https://doi.org/10.1016/j.scitotenv.2016.04.012
Custódio D, Cerqueira M, Alves C, Nunes T, Pio C, Esteves V, Frosini D, Lucarelli F, Querol X (2016) A one-year record of carbonaceous components and major ions in aerosols from an urban kerbside location in Oporto, Portugal. Sci Total Environ 562:822–833. https://doi.org/10.1016/j.scitotenv.2016.04.012
Dao X, Wang Z, Lv Y, Teng E, Zhang L, Wang C (2014) Chemical characteristics of water-soluble ions in particulate matter in three metropolitan areas in the North China Plain. PLoS One 9:e113831. https://doi.org/10.1371/journal.pone.0113831
Deshmukh DK, Deb MK, Tsai YI, Mkoma SL (2010) Atmospheric ionic species in PM 2.5 and PM 1 aerosols in the ambient air of eastern central India. J Atmos Chem 66(81). https://doi.org/10.1007/s10874-011-9194-1
Flores RM, Mertoglu E, Ozdemir H, Akkoyunlu BO, Demir G, Unal A, Tayanc M (2020a) A high-time resolution study of PM2.5, organic carbon, and elemental carbon at an urban traffic site in Istanbul. Atmos Environ 223:117241. https://doi.org/10.1016/j.atmosenv.2020.117241
Flores RM, Özdemir H, Akkoyunlu BO, Ünal A, Tayanç M (2020b) Seasonal variation of carbonaceous PM2.5 in an Istanbul traffic site. Atmos Pollut Res 11:2110–2118. https://doi.org/10.1016/j.apr.2020.06.022
Flores RM, Özdemir H, Ünal A, Tayanç M (2022) Distribution and sources of SVOCs in fine and coarse aerosols in the megacity of Istanbul. Atmos Res 271:106100. https://doi.org/10.1016/j.atmosres.2022.106100
Gao XM, Yang LX, Cheng SH, Gao R, Zhou Y, Xue LK, Shou YP, Wang J, Wang XF, Nie W, Xu PJ, Wang WX (2011) Semi-continuous measurement of water-soluble ions in PM2.5 in Jinan, China: temporal variations and source apportionments. Atmos Environ 45:6048–6056. https://doi.org/10.1016/j.atmosenv.2011.07.041
Gao ZX, Wang XL, Shen LJ, Xiang H, Wang HL (2019) Characteristics of aerosol chemical compositions and size distributions during a long-range dust transport episode in an urban city in the Yangtze River Delta. Atmosphere 10:68. https://doi.org/10.3390/atmos10020068
He L, Chen H, Rangognio J, Yahyaoui A, Colin P, Wang JH, Daele V, Mellouki A (2018) Fine particles at a background site in Central France: chemical compositions, seasonal variations and pollution events. Sci Total Environ 612:1159–1170. https://doi.org/10.1016/j.scitotenv.2017.08.273
Hong Y, Li C, Li X, Ma Y, Zhang Y, Zhou D, Wang Y, Liu N, Chang X (2018) Analysis of compositional variation and source characteristics of water-soluble ions in PM2. 5 during several winter-haze pollution episodes in Shenyang, China. Atmosphere 9(280)
Hopke PK (2003) Recent developments in receptor modeling. J Chemom 17:255–265. https://doi.org/10.1002/cem.796
Im U, Markakis K, Unal A, Kindap T, Poupkou A, Incecik S, Yenigun O, Melas D, Theodosi C, Mihalopoulos N (2010) Study of a winter PM episode in Istanbul using the high resolution WRF/CMAQ modeling system. Atmos Environ 44:3085–3094. https://doi.org/10.1016/j.atmosenv.2010.05.036
Indris SN, Rudolph DL, Glass BK, Cappellen PV (2020) Evaluating phosphorous from vehicular emissions as a potential source of contamination to ground and surface water. Cogent Environ Sci 6:1794702. https://doi.org/10.1080/23311843.2020.1794702
Jain S, Sharma SK, Vijayan N, Mandal TK (2020) Seasonal characteristics of aerosols (PM2.5 and PM10) and their source apportionment using PMF: a four year study over Delhi. India Environ Pollut 262(114337). https://doi.org/10.1016/j.envpol.2020.114337
Javed W, Wexler AS, Murtaza G, Ahmad HR, Basra SMA (2015) Spatial, temporal and size distribution of particulate matter and its chemical constituents in Faisalabad, Pakistan. Atmosfera 28:99–116. https://doi.org/10.1016/S0187-6236(15)30003-5
Jiang N, Yin SS, Guo Y, Li JY, Kang PR, Zhang RQ, Tang XY (2018) Characteristics of mass concentration, chemical composition, source apportionment of PM2.5 and PM10 and health risk assessment in the emerging megacity in China. Atmos Poll Res 9:309–321. https://doi.org/10.1016/j.apr.2017.07.005
Kanakidou M, Mihalopoulos N, Kindap T, Im U, Vrekoussis M, Gerasopoulos E, Dermitzaki E, Unal A, Kocak M, Markakis K, Melas D, Kouvarakis G, Youssef AF, Richter A, Hatzianastassiou N, Hilboll A, Ebojie F, Wittrock F, von Savigny C et al (2011) Megacities as hot spots of air pollution in the East Mediterranean. Atmos Environ 45:1223–1235. https://doi.org/10.1016/j.atmosenv.2010.11.048
Karaca M, Tayanc M, Toros H (1995) Effects of urbanization on climate of Istanbul and Ankara. Atmos Environ 29:3411–3421. https://doi.org/10.1016/1352-2310(95)00085-D
Krzyzanowski M, Apte JS, Bonjour SP, Brauer M, Cohen AJ, Prüss-Ustun AM (2014) Air pollution in the mega-cities. Curr Env Health Rep 1:185–191. https://doi.org/10.1007/s40572-014-0019-7
Lai SC, Zou SC, Cao JJ, Lee SC, Ho KF (2007) Characterizing ionic species in PM2.5 and PM10 in four Pearl River Delta cities, south China. J Environ Sci (China) 19:939–947. https://doi.org/10.1016/s1001-0742(07)60155-7
Lee H-M, Lee SP, Li Y, Yu JZ, Kim JY, Kim YP, Lee JY (2021) Characterization of seasonal difference of HULIS-C sources from water soluble PM2.5 in Seoul, Korea: probing secondary processes. Aerosol and Air Quality Research 21:200233. https://doi.org/10.4209/aaqr.2020.05.0233
Lin JJ (2002) Characterization of water-soluble ion species in urban ambient particles. Environ Int 28:55–61. https://doi.org/10.1016/s0160-4120(02)00004-1
Şahin ÜA, Onat B, Akın Ö, Ayvaz C, Uzun B, Mangır N, Doğan M, Harrison RM (2020) Temporal variations of atmospheric black carbon and its relation to other pollutants and meteorological factors at an urban traffic site in Istanbul. Atmos Pollut Res. https://doi.org/10.1016/j.apr.2020.03.009
Shen ZX, Cao JJ, Arimoto R, Han ZW, Zhang RJ, Han YM, Liu SX, Okuda T, Nakao S, Tanaka S (2009) Ionic composition of TSP and PM2.5 during dust storms and air pollution episodes at Xi'an, China. Atmos Environ 43:2911–2918. https://doi.org/10.1016/j.atmosenv.2009.03.005
Shi JH, Wang N, Gao HW, Baker AR, Yao XH, Zhang DZ (2019) Phosphorus solubility in aerosol particles related to particle sources and atmospheric acidification in Asian continental outflow. Atmos Chem Phys 19:847–860. https://doi.org/10.5194/acp-19-847-2019
Shon ZH, Kim KH, Song SK, Jung K, Kim NJ, Lee JB (2012) Relationship between water-soluble ions in PM2.5 and their precursor gases in Seoul megacity. Atmos Environ 59:540–550. https://doi.org/10.1016/j.atmosenv.2012.04.033
Silvern RF, Jacob DJ, Kim PS, Marais EA, Turner JR, Campuzano-Jost P, Jimenez JL (2017) Inconsistency of ammonium–sulfate aerosol ratios with thermodynamic models in the eastern US: a possible role of organic aerosol. Atmos Chem Phys 17:5107–5118. https://doi.org/10.5194/acp-17-5107-2017
Spencer MT, Shields LG, Sodeman DA, Toner SM, Prather KA (2006) Comparison of oil and fuel particle chemical signatures

with particle emissions from heavy and light duty vehicles. Atmos Environ 40:5224–5235. https://doi.org/10.1016/j.atmosenv.2006.04.011

Tsai JH, Tsai SM, Wang WC, Chiang HL (2016) Water-soluble ionic species of coarse and fine particulate matter and gas precursor characteristics at urban and rural sites of central Taiwan. Environ Sci Pollut Res 23:16722–16737. https://doi.org/10.1007/s11356-016-6834-7

Tsai YI, Sopajaree K, Kuo SC, Hsin TY (2015) Chemical composition and size-fractionated origins of aerosols over a remote coastal site in Southern Taiwan. Aerosol Air Qual Res 15:2549–2570. https://doi.org/10.4209/aaqr.2015.09.0566

Tutsak E, Kocak M (2019) High time-resolved measurements of water-soluble sulfate, nitrate and ammonium in PM2.5 and their precursor gases over the Eastern Mediterranean. Sci Total Environ 672:212–226. https://doi.org/10.1016/j.scitotenv.2019.03.451

Tutsak E, Koçak M (2019) High time-resolved measurements of water-soluble sulfate, nitrate and ammonium in PM2.5 and their precursor gases over the Eastern Mediterranean. Sci Total Environ 672:212–226. https://doi.org/10.1016/j.scitotenv.2019.03.451

Uria-Tellaetxe I, Carslaw DC (2014) Conditional bivariate probability function for source identification. Environ Model Softw 59:1–9. https://doi.org/10.1016/j.envsoft.2014.05.002

Venkataraman C, Chandramouli B, Patwardhan A (1999) Anthropogenic sulphate aerosol from India: estimates of burden and direct radiative forcing. Atmos Environ 33:3225–3235. https://doi.org/10.1016/S1352-2310(98)00140-X

Wang Y, Zhuang GS, Zhang XY, Huang K, Xu C, Tang AH, Chen JM, An ZS (2006) The ion chemistry, seasonal cycle, and sources of PM2.5 and TSP aerosol in Shanghai. Atmos Environ 40:2935–2952. https://doi.org/10.1016/j.atmosenv.2005.12.051

Wei N, Xu Z, Liu J, Wang G, Liu W, Zhuoga D, Xiao D, Yao J (2019) Characteristics of size distributions and sources of water-soluble ions in Lhasa during monsoon and non-monsoon seasons. J Environ Sci (China) 82:155–168. https://doi.org/10.1016/j.jes.2019.02.017

Ye ZL, Liu JS, Gu AJ, Feng FF, Liu YH, Bi CL, Xu JZ, Li L, Chen H, Chen YF, Dai L, Zhou QF, Ge XL (2017) Chemical characterization of fine particulate matter in Changzhou, China, and source apportionment with offline aerosol mass spectrometry. Atmos Chem Phys 17:2573–2592. https://doi.org/10.5194/acp-17-2573-2017

Zhang X, Ji G, Peng X, Kong L, Zhao X, Ying R, Yin W, Xu T, Cheng J, Wang L (2022) Characteristics of the chemical composition and source apportionment of PM2.5 for a one-year period in Wuhan, China. J Atmos Chem. https://doi.org/10.1007/s10874-022-09431-6

Zhang X, Zhao X, Ji G, Ying R, Shan Y, Lin Y (2019) Seasonal variations and source apportionment of water-soluble inorganic ions in PM 2.5 in Nanjing, a megacity in southeastern China. J Atmos Chem 76:73–88

Zhao JP, Zhang FW, Xu Y, Chen JS (2011) Characterization of water-soluble inorganic ions in size-segregated aerosols in coastal city, Xiamen. Atmos Res 99:546–562. https://doi.org/10.1016/j.atmosres.2010.12.017

Zhao M, Qiao T, Huang Z, Zhu M, Xu W, Xiu G, Tao J, Lee S (2015) Comparison of ionic and carbonaceous compositions of PM2.5 in 2009 and 2012 in Shanghai, China. Sci Total Environ 536:695–703. https://doi.org/10.1016/j.scitotenv.2015.07.100